npj | Flexible Electronics

www.nature.com/npjflexelectron

ARTICLE OPEN

On the unipolarity of charge transport in methanofullerene diodes

Ardalan Armin[1,2], Safa Shoaee[1,3], Qianqian Lin[1,4], Paul L Burn[1] and Paul Meredith[1,5]

Fullerenes are electron transporting organic semiconductors with a wide range of applications. In particular, methanofullerenes have been the preferred choice for solution-processed solar cells and photodiodes. The wide applicability of fullerenes as both '*n*-type' transport materials and electron acceptors is clear. However, what is still a matter of debate is whether the fullerenes can also support efficient transport of holes, particularly in diode geometries. In this letter, we utilize a number of recently developed experimental methods for selective electron and hole mobility measurements. We show for the two most widely used solution processable fullerenes, PC70- and-PC60BM, that whilst both exhibit electron mobilities as high as 10^{-3} cm^2/Vs, their hole mobilities are < 10^{-9} cm^2/Vs. Thus charge transport in these fullerenes can be considered predominantly unipolar in diode configurations.

npj Flexible Electronics (2017)1:13 ; doi:10.1038/s41528-017-0012-y

INTRODUCTION

The methanofullerenes, PCXBM (phenyl-C_X-butyric acid methyl ester where $X = 60$ or 70), have seen widespread use in organic solar cells and photodiodes. They are also used as '*n*-type' transport layers in hybrid optoelectronics such as nanocrystal diodes[1] or organohalide perovskite solar cells.[2] In spite of the great success of the methanofullerene semiconductors in delivering state-of-the-art device performance metrics in specific applications, a number of fundamental issues concerning the solid-state physics of films of the materials remain unclear. In particular, an adequate understanding of the charge transporting properties is still a matter of significant importance.

Models based upon hopping of carriers between localized states are normally used to describe charge transport in disordered semiconductors.[3] A direct consequence of hopping transport is that electrons and holes may experience significantly different potential landscapes over their respective transport pathways, i.e., the potential landscapes for the lowest unoccupied molecular orbitals (LUMOs – for an electron) and the highest occupied molecular orbitals (HOMOs – for the hole) can involve localization of states with different potential depths (trap states) and/or energetic disorder. This simple construct is often advanced as the possible explanation for predominantly unipolar hole transport in many organic semiconductors,[4] where the electrons are deeply trapped and hence localized. For example, Nicolai et al.[5] have shown that in polymer semiconductors deep traps for the electrons are the reason behind their often observed poor and dispersive electron transport whilst they can exhibit relatively trap-free hole mobility.[6] Wetzelaer et al., however, have shown that in two specific "*n*-type" polymers the scenario is the reverse, with superior electron to hole mobility observed.[7] They attributed the origin of such imbalance in the transport to different reorganization energies for electron (reduction) and hole (oxidation) transport and hopping transfer integrals. However, whether a material is perceived to be unipolar (i.e., able to conduct only one type of carrier) or bipolar, can be strongly dependent on the experiment used to measure the hole and electron mobilities. In this context, there have been a number of reports of experimental measurements that show organic semiconductors traditionally thought to be only hole transporters can in fact be bipolar.[6, 8, 9] Indeed, for most organic semiconductors, there is no theoretical reason why they should not support the transport of both carrier types providing charges can be injected or extracted via a suitable contact.

The question of bipolar transport is equally valid for those materials traditionally thought to be electron transport materials. For example, the fullerenes are often considered to only transport electrons. Thus, following traditional semiconductor nomenclature, they are often referred to as being '*n*-type', although strictly speaking these materials are un-doped and this short-hand is therefore not completely accurate. Irrespective of the nomenclature, fullerenes possess high electron affinities ~3.7–4.2 eV in relation to many other organic semiconductors, and hence are considered strong electron acceptors in a variety of applications. Thus elucidating the charge mobility characteristics in fullerene containing films is important given their common usage as electron acceptors in organic solar cells (OSCs), electron transport interlayers in high efficiency organohalide perovskite solar cells,[2] and as a hole blocking layer in ultra-low noise organic[10] and organohalide perovskite photodiodes.[11] In this article we present measurements that allow independent determination of electron and hole mobilities in neat PCBM diode structures, under what may be considered operational conditions for solar cells and photodiodes. The measurements show that in a diode

[1]Centre for Organic Photonics & Electronics, The University of Queensland, St Lucia Campus, Brisbane, QLD 4072, Australia
Correspondence: Ardalan Armin (a.armin@uq.edu.au) or Paul Meredith (meredith@physics.uq.edu.au)
[2]Present address: Centre for Engineered Quantum Systems, School of Mathematics and Physics, The University of Queensland, St Lucia Campus, Brisbane, QLD 4072, Australia
[3]Present address: Institute of Physics and Astronomy, University of Potsdam, Karl-Liebknecht-Straße 24-25, Potsdam-Golm D-14476, Germany
[4]Present address: Clarendon Laboratory, Department of Physics, The University of Oxford, Parks Road Oxford, Oxford, OX1 3PU, UK
[5]Present address: Department of Physics, Swansea University, Singleton Park, Swansea, Wales SA2 8PP, UK

Received: 6 November 2016 Revised: 16 July 2017 Accepted: 15 August 2017
Published online: 18 December 2017

configuration the PCBMs have essentially unipolar character with an electron mobility of $(1.0 \pm 0.2) \times 10^{-3}$ cm^2/Vs in agreement with previous reports,[12] but in contrast their hole mobility is $< 10^{-9}$ cm^2/Vs.

RESULTS

Selective electron and hole mobility measurements using injected charges (MIS-CELIV)

In order to evaluate the carrier mobilities in a neat PC70BM or PC60BM films, we used metal-insulator-semiconductor (MIS) diodes in combination with charge extraction in linearly increasing voltage (CELIV).[13] To this end, two series of hole-only and electron-only MIS diodes were prepared. The device structure was glass/ITO 80 nm/MgF_2 70 nm/PC70BM or PC60BM and then MoO_x/Ag for hole-only devices and an Al electrode for the electron-only MIS devices. As shown in Fig. 1a, a triangular CELIV voltage pulse was applied to the device with an offset voltage V_{off} such that in the case of the hole mobility measurements, the MoO_x/Ag electrode is initially positive ($t < 0$) allowing for hole injection whilst for the electron-only devices, $V_{off} > 0$ with respect to the ITO electrode. The larger the offset, the greater the number of injected carriers that accumulate at the interface ($t < 0$). Subsequently, the triangular voltage extracts the carriers and therefore during extraction ($t > 0$), the larger offsets result in higher currents, and the transit time and mobility are measured from the current transient as described previously.[13] A PC70BM diode with structure glass/ITO/PC70BM/Al was also prepared for photo-CELIV measurements, which uses a laser pulse instead of an offset voltage to create the carriers in the device. Figure 1b shows the current transient for the photo-CELIV experiment performed on a PC70BM diode pumped with a short laser pulse at a wavelength of 355 nm. The photogenerated carriers were then extracted by the triangular voltage pulse in reverse bias.[14] The faster carrier mobility can be calculated from photo-CELIV to be

$$\mu_f = \frac{2d^2}{3At_{max}^2\left[1 + 0.36\frac{\Delta j}{j_0}\right]} \quad (1)$$

where d is the junction thickness, j_0 the displacement current of the capacitor (the diode), Δj is the difference between the maximum extraction current measured at t_{max} and j_0, and $A = V_{max}/t_p$ the voltage slope with V_{max} and t_p being the amplitude and length of the voltage pulse. It is important to note that photo-CELIV cannot distinguish between electrons and holes, rather it only measures the faster carrier mobility regardless of their type. We measured a faster carrier mobility of $(2.0 \pm 0.4) \times 10^{-3}$ cm^2/Vs using photo-CELIV which is in agreement with the electron mobilities previously reported for PC70BM containing films.[15, 16] Using a MgF_2 insulator layer between the organic film and the ITO prevents hole injection into the PC70BM layer so that only electron injection occurs when the Al electrode is positively biased. Figure 1c and e show the MIS-CELIV current transients as a function of offset voltage for PC70BM and PC60BM devices, respectively. By increasing the offset, Δj increases until the electric field becomes screened during the extraction when the initially injected carriers form space charges. In such a case, the current reaches a secondary displacement current corresponding to the capacitance of the MgF_2 layer since the PCBM layer is screened by space charges. In this case, the transit time can be evaluated from the time at which the current reaches $2j_0$ as described by

$$t_{tr} = \frac{4}{\pi} t_{2j0}, \quad (2)$$

and the charge carrier mobility can be calculated from the transit time in the MIS-diode[13]

$$\mu = \frac{2d^2}{At_{tr}^2}\left(1 + \frac{\epsilon d_i}{\epsilon_i d}\right) \quad (3)$$

where d_i is the insulating layer thickness, ϵ_i its dielectric constant, ϵ the active layer dielectric constant and A the voltage ramp.

From these MIS-CELIV measurements we determined an electron mobility of $(1.0 \pm 0.2) \times 10^{-3}$ cm^2/Vs for both PC60BM and PC70BM–a value very close to that measured by photo-CELIV. A slight difference between photo- and MIS-CELIV values is anticipated since MIS-CELIV uses a thin sheet of induced carriers when the applied offset voltage $U_{offset} \gg kT/e$ with a distribution density function $\rho(y)$ given by the solution to the Poisson equation[13]

$$\rho(y) = \rho(0)\left(1 + \frac{eU_{offset}}{2kT}\frac{y}{d_i}\right)^{-2} \quad (4)$$

whilst in the case of photo-CELIV, the carriers are distributed in the bulk, based upon the optical field distribution in the diode cavity. In the above equation, k is the Boltzmann's constant, T the absolute temperature, y the coordinate perpendicular to the electrode surfaces measured from the insulator-semiconductor interface, e the electron charge, and $\rho(0)$ the charge carrier density at the interface of the insulator/semiconductor. We then reversed the polarity of the experiment and used a hole-only device in an attempt to observe hole transport in films of PC70BM and PC60BM. In this case, the ITO electrode is negatively biased and the MgF_2 insulating layer blocks electron injection, with the MoO_x/Ag designed to inject holes. We note that MoO_x has been reported to have a variety of different work functions depending on the method of deposition and subsequent treatment, e.g., exposure to air or thermal annealing.[17, 18] Freshly deposited MoO_x has been reported to have a work function of >6 eV,[17, 18] which is sufficient to inject holes into PCBM with an ionization potential of ~6 eV.[19] Hence, in this work we deposited the MoO_x films, completed the structure and performed the measurements immediately to ensure the MoO_x work function was as large as possible. Figure 1d and f show that in contrast to the electron-only devices, there is no extraction current in the hole-only fullerene devices at any offset voltage.

However, we acknowledge that in spite of best efforts it is possible that the deposited MoO_x layer may have a work function <6 eV such that there could be a barrier to hole injection.[20] Therefore, as a further check of our results, we used an alternative method that is not reliant on Ohmic contacts. The data reported in Fig. 1 from MIS-CELIV shows that the carrier mobilities are similar for both PC60BM and PC70BM and as such, the latter part of the study focused on PC70BM films.

Selective electron and hole mobility measurement using photogenerated charges (photo-MIS-CELIV)

To further elucidate the mobilities of PC70BM film-based diodes we performed photo-MIS-CELIV. This newly developed technique benefits from the selectivity of MIS-CELIV, and also takes advantage of photo-CELIV in that charge extraction is independent of the work function of the electrodes. As such, photo-MIS-CELIV can confirm that an absence of an extracted hole current is not due to any injection barrier into PC70BM. Figure 2a schematically shows the pulse synchronization of the Photo-MIS-CELIV measurement. It should be noted that the LED ON time is for a time period much longer than the CELIV pulse length t_p. The LED operates at a wavelength of 550 nm and irradiance of 2 mW/cm^2. The Photo-MIS-CELIV experiments were performed using electron- and hole-only MIS-diodes (active layer thickness 500–700 nm) and we re-iterate that the initial carriers were photogenerated rather than injected. In the photo-MIS-CELIV

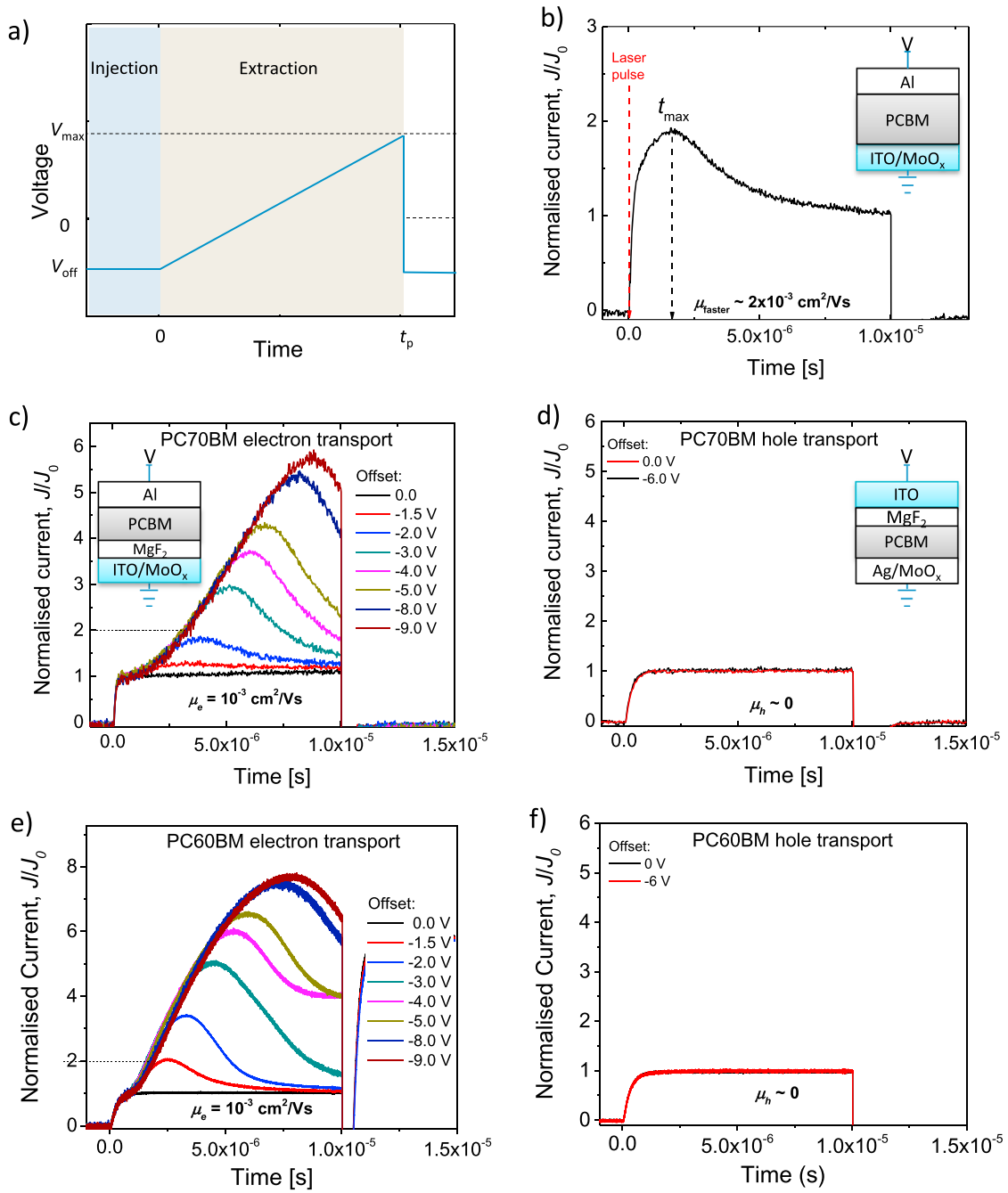

Fig. 1 Photo-CELIV and MIS-CELIV experimental results for PC70BM and PC60BM. **a** A schematic of the pulse shape used in photo- and MIS-CELIV measurements. At $t < 0$ a negative offset is applied to the device (forward bias) allowing injection of carriers (only for MIS-CELIV) and $t > 0$ the triangle voltage pulse extracts the injected carriers. **b** Photo-CELIV transient for a PC70BM diode structure is shown in the inset. The faster carrier mobility is measured, as photo-CELIV is insensitive to the slower carrier mobility. **c** MIS-CELIV transient for an electron-only diode shown with its biasing conditions in the inset. The measured electron mobility is in agreement with photo-CELIV. **d** MIS-CELIV transients for a hole-only diode showing no hole mobility can be detected for PC70BM. MIS-CELIV transients of PC60BM are shown in **e** and **f** for electron and hole only devices, respectively

experiment for electron mobility measurements, a hole-only device was used (ITO/MgF_2/fullerene/MoO_x/Ag), and the MoO_x/Ag electrode was negatively biased during the light exposure with an LED for ~500 ms. During the light exposure, the work function of the electrode is not low enough to inject electrons, however, a fraction of photogenerated excitons can be dissociated at the electrode; leaving electrons behind in the bulk and holes transferred to the negatively biased MoO_x/Ag electrode. If the fullerene diode were able to support hole transport, then the photogenerated holes in the bulk could drift to the negatively biased electrode resulting in accumulation of electrons at the MgF_2/semiconductor interface. The electrons would then be extracted by the MoO_x/Ag electrode as it becomes positively biased relative to the initial bias (during the triangular voltage pulse period). Using this photo-MIS-CELIV technique we again obtain an electron mobility of $(1.0 \pm 0.2) \times 10^{-3}$ cm^2/Vs (Fig. 2b). The extraction current shown in Fig. 2b confirms that electrons were extracted from the MoO_x/Ag electrode despite it being far

from an Ohmic contact for electrons due to the substantial difference between the electron affinities of PC70BM (~4.1 eV) and the MoO_x/Ag electrode (~ 6 eV). When the measurements were performed in the dark, we found no injection of electrons as expected for the MoO_x/Ag electrode. Using this photo-MIS-CELIV technique we obtained no signal corresponding to hole extraction as shown in Fig. 2c. The measurement for holes was conducted on ITO/MgF_2/fullerene/Al in which the Al electrode was positively biased during the light exposure, extracting the electrons. In strong contrast with the MoO_x/Ag electrode, any accumulated holes did not give rise to an extraction current. These results are consistent with our MIS-CELIV and photo-CELIV findings, and provide further evidence for the proposition that in these neat PCBM diodes, we observe no measurable hole transport. We would note that our instrument resolution limit (voltage pulse length of 1 µs to 100 ms) enables us to access a mobility range from 1 cm^2/Vs to 10^{-9} cm^2/Vs–the latter therefore representing the upper limit of hole mobility in the film.

The impact of illumination inversion in a neat PC70BM film solar cell

Finally, we consider how the above results impact operational device performance by comparing conventional and illumination inverted PC70BM solar cells. It should be noted that this is an additional cross-check of the transient-current-based findings. By manipulating the electro-optics of the diode, i.e., changing the electron and hole transport polarity, it is possible to change the direction of electron and hole extraction. We fabricated conventional and inverted thick PC70BM devices as shown in Fig. 3a. The PC70BM was deliberately made thick (800 nm) to achieve a large optical density (*ad*), which results in most of the photogeneration occurring near the electrode on the illumination side.[21] When illuminated from the anode side (conventional configuration), the carriers are photogenerated closer to the hole extracting electrode and their average travel distances can be written as

$$\langle x_h \rangle = \frac{\int_0^d x e^{-\langle \alpha \rangle x} dx}{\int_0^d e^{-\langle \alpha \rangle x} dx} \approx 1/a \quad (5)$$

and therefore

$$\langle x_e \rangle \approx d \quad (6)$$

when *ad* is sufficiently large. This implies that the transit time of holes will be very short regardless of their (low) mobility while electrons must traverse the entire film thickness to reach the cathode. The corresponding photo-response in Fig. 3b shows that carrier photogeneration and extraction occurs, and a measurable peak external quantum efficiency of 1.5% is achieved at 350 nm. We attribute this photocurrent (although quite modest) to exciton generation and diffusion within a thin layer 10–20 nm near the ITO electrode. In contrast, illumination through the cathode (inverted configuration) generates no photo-response as shown in Fig. 3b, which again indicates poor hole transport stemming from the fact that the average travel distance for the holes $\langle x_h \rangle$ in this case is $\approx d$ (in analogy with the conventional case, Eqs. 5 and 6). The significant difference between the conventional and inverted cases, once again confirms that hole transport is not supported in these neat PCBM diodes.

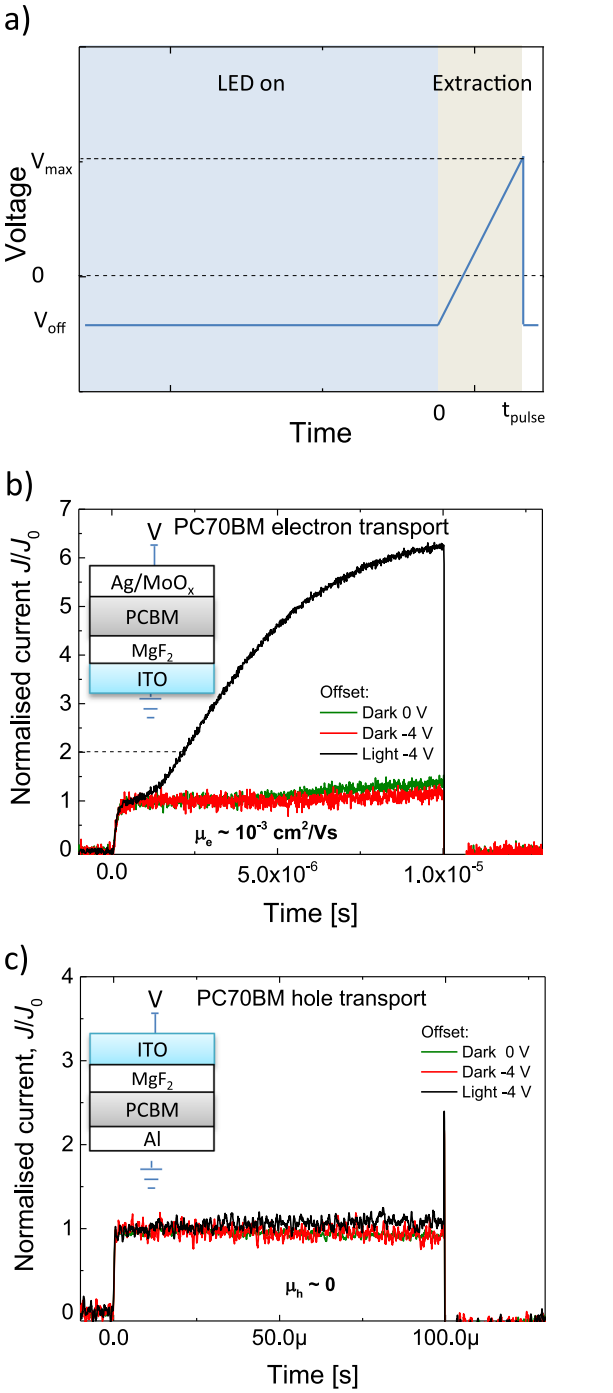

Fig. 2 Photo-MIS-CELIV experiment for electron and hole mobility measurements on PC70BM diodes. Schematic of the voltage and LED pulses are shown in **a**. **b** Raw photo-MIS-CELIV signals for an electron mobility measurement. For this purpose, a hole-only device is used to prevent the initial injection of electrons. The measured value for electron mobility is in agreement with photo-CELIV and MIS-CELIV. **c** Photo-MIS-CELIV signals for hole measurement in PC70BM diodes showing no measurable hole transport. Insets: Hole only **b** and electron only **c** device configurations employed

DISCUSSION

Numerous publications have reported electron and hole mobilities of different organic solar cell BHJ systems vs. the fraction of electron acceptor (fullerene) in order to investigate the role of the electron-hole mobility ratio,[22] or optimize the composition with respect to power conversion efficiency.[23] For example, Tuladhar et al.[12] reported that hole mobilities increased for a BHJ film, and postulated that hole transport in the fullerene could play a role in this observation. It is worthy of note that the overall macroscopic electron and hole mobilities as measured in this case[12], could well be different to the local mobility of a single component within a

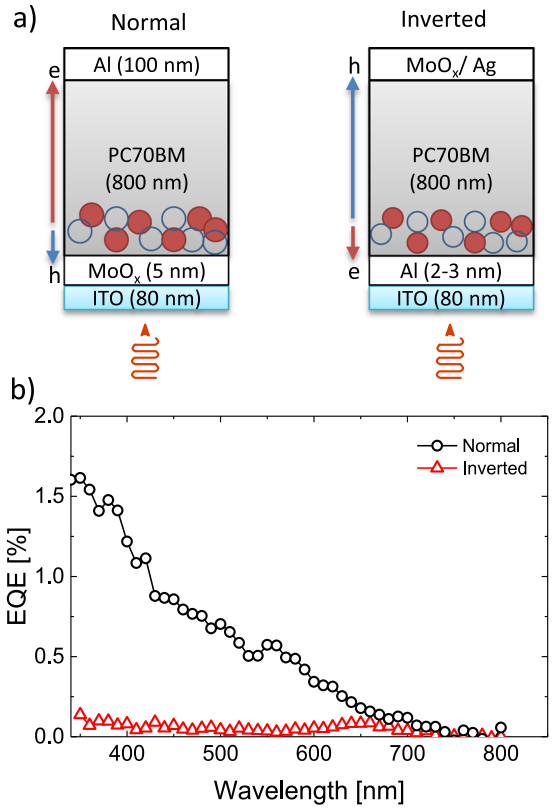

Fig. 3 **a** Schematics of conventional and electrically inverted solar cell structures with an 800 nm thick layer of PC70BM. **b** EQE response of conventional and inverted structures at short circuit current. The conventional device shows a photoresponse whilst the inverted has negligible EQE. In the conventional geometry the holes are generated very close to the anode whilst in the inverted structure they must travel across the entire active layer thickness due to the large optical density of the thick PC70BM film

multi-component system. This question has recently been addressed by Burke et al.[24] and Bartelt et al.[25] who investigated the effect of fullerene percolation in a mixed acceptor:donor phase and assessed its impact on charge generation in an organic solar cell blend. However, the strongest evidence for hole transport in fullerenes is the work of Anthopoulos et al.[16] who reported a field effect hole mobility of 2×10^{-5} cm^2/Vs for PC70BM films in a field effect transistor (FET) architecture. It is not however clear whether this FET-based observation has general relevance to all possible device configurations, notably diodes.

Our selective electron and hole mobility measurements for the neat PC60BM and PC70BM diodes shows that the bulk hole mobility of these methanofullerene is orders of magnitude lower than that of electrons and below the limit of the measurement, 10^{-9} cm^2/Vs. We have also introduced photo-MIS-CELIV as a method to selectively quantify charge carrier mobilities independent of injection barrier considerations, and once again find no observable hole transport.

The possible differences between electron and hole transport in disordered semiconductors is still a relatively unexplored subject in solid state physics. In analogy with the work of Wetzelaer et al.,[7] strong imbalance of the electron/hole mobility of an organic semiconductor could potentially originate from asymmetry in the parameters that define the hopping rate within the framework of Marcus–Hush theory. The hopping rate from site i to j with energies ϵ_i and ϵ_j can be written as

$$\nu_{ij} = \nu_0 \exp\left(-\frac{E_a}{kT}\right) \exp\left[-\frac{\epsilon_j - \epsilon_i}{2k_BT} - \frac{(\epsilon_j - \epsilon_i)^2}{16E_ak_BT}\right]; \quad (7)$$

$$\nu_0 = I_{ij}^2/\hbar\sqrt{\pi/4E_akT} \quad (8)$$

where the first exponent term denotes the polaron activation, which is defined as $E_a = \lambda/4$, where λ is the reorganization energy for either electron or hole transport. I_{ij}^2 is the transfer integral and the rest of the symbols have their usual meaning. The possible differences in the hopping rate ν_{ij} for electron and hole transport can originate from: (i) Different internal reorganization energies for moving from the neutral to the oxidized or reduced species and vice versa. The internal reorganization energy is dependent on the changes in the geometry of the two molecules when going from an initial to a final state. The initial and final species are different for hole and electron transport leading to the reorganization energy being previously shown to be different in organic semiconductors–inducing imbalance in electron and hole mobilities;[7] (ii) Asymmetry in the transfer integrals for electron and hole transfer. It has been shown that due to the different spatial distribution of the HOMO and LUMO orbitals in organic molecules, the wavefunction overlap and thereby transfer integral can be substantially different for electron and hole transfer between molecules;[7, 26] (iii) Different disordered landscapes for electrons and holes. Marcus–Hush theory and the Gaussian Disorder Model (GDM)[27] have been applied to a 3D network of molecules with energetic disorder σ.[28] The charge carrier mobility is dependent on energetic disorder σ as follows

$$\mu \propto \exp\left[c\left(\frac{\sigma}{k_BT}\right)^2\right], \quad (9)$$

in which c is a constant and σ plays a significant role in defining the carrier transport. At this stage it has not been possible to selectively measure σ for the HOMO and LUMO orbitals, and it would be bold to assume that they have identical energetic disorder. Thus, it is likely that the electrons and holes experience different disordered potential landscapes during the multiple hopping processes that occur through the bulk resulting in different electron and hole mobilities.

Finally we note that the exact reason behind the strong mobility imbalance in the charge transport properties of methanofullerenes will require further system-specific investigation across a range of differently substituted fullerenes, and selective quantification of reorganization energy, transfer integrals for electron and hole transport, as well as determining energetic disorder of the HOMO and LUMO states.

METHODS

Device fabrication

ITO was pre-patterned and purchased from Kintec, and MgF_2, MoO_x, Ag and Al were deposited by thermal evaporation under a vacuum of 10^{-6} mbar. PC70BM and PC60BM were purchased from American Dye Source. PC70BM was deposited by spin-coating in a nitrogen atmosphere (O_2 and H_2O <1 p.p.m.) from anhydrous chloroform solution containing 10% 1,2-dichlorobenzene by volume at a concentration of 50 mg/mL and spin rate of 600 RPM, while PC60BM was deposited by spin-coating from a hot chloroform solution (60 °C) at a concentration of 50 mg/mL and spin rate of 500 RPM. These processing conditions should in principle minimize the amount of oxygen incorporated into the films during deposition. The area of devices used in CELIV experiment was 0.04 cm^2. The small-size sample ensured short parasitic *RC*-time constant in the circuit.

CELIV

The general CELIV experimental method is reported elsewhere.[13, 29] For MIS-CELIV, a delay generator (Stanford Research System DG535) and an arbitrary

waveform generator (Agilent 33250 A) were used to generate the CELIV triangle pulse. For photo-CELIV a delay generator (Stanford Research System DG535) was also used for pulse synchronization along with a Q-switched second-harmonic Nd:YAG laser (Quantel Brio) working at a wavelength of 532 nm and pulse duration of 5 ns. The signal was recorded using a digital storage oscilloscope (LeCroy Waverunner A6200). The *RC*-time of the circuit was less than 200 ns. 6 devices were examined for each measurement and no significant device-to-device variations were identified in the transients.

External quantum efficiency

The EQE was measured using a PV Measurements Inc QEX7 setup operating at 120 Hz and electrical bandwidth of approximately 1 Hz. 6 pixels were tested for this measurements.

Statistics

Reported mobilities were calculated from the transit times and device thickness. The mobility precision was approximately 12% (one standard deviation) calculated from the propagation of uncertainties of the transit time (10%) and the device thickness (5%). Six devices were tested for each measurement and the mobility values were within two standard deviation of the mean.

Data availability

The datasets generated during and/or analyzed during the current study are available from the corresponding author on reasonable request.

ACKNOWLEDGEMENTS

The authors wish to thank Ivan Kassal for fruitful discussions. The project has been supported by the Australian Government through the Australian Renewable Energy Agency (ARENA) and Australian Centre for Advanced Photovoltaics (ACAP). Responsibility for the views, information or advice expressed herein is not accepted by the Australian Government. A.A. is now a Sêr Cymru Rising Star senior fellow. P.M. is currently a Sêr Cymru Research Chair. S.S. is now a Sofja Kovalevskaja awardee of Alexander von Humboldt Foundation. P.L.B. was a University of Queensland Vice Chancellor's Research Focused Fellow and is currently an ARC Laureate Fellow (FL160100067). This work was performed in part at the Queensland node of the Australian National Fabrication Facility (ANFF-Q): a company established under the National Collaborative Research Infrastructure Strategy to provide nano and micro fabrication facilities for Australia's researchers.

AUTHOR CONTRIBUTIONS

A.A. conceptualized the research work. A.A. and Q.L. performed the measurements. A. A. analysed the results and A.A., S.S., Q.L., and P.M. interpreted them. A.A. wrote the manuscript which was further improved by S.S. and P.M. and then equally optimized by co-authors. All authors have given approval of the final submission.

ADDITIONAL INFORMATION

Competing interests: The authors declare that they have no competing financial interests.

Publisher's note: Springer Nature remains neutral with regard to jurisdictional claims in published maps and institutional affiliations.

REFERENCES

1. Yuan, M., Voznyy, O., Zhitomirsky, D., Kanjanaboos, P. & Sargent, E. H. Synergistic doping of fullerene electron transport layer and colloidal quantum dot solids enhances solar cell performance. *Adv. Mater.* **27**, 917–921 (2015).
2. Malinkiewicz, O. et al. Perovskite solar cells employing organic charge-transport layers. *Nat. Photon.* **8**, 128–132 (2014).
3. Baranovskii, S. Theoretical description of charge transport in disordered organic semiconductors. *Phys. Status Solidi (B)* **251**, 487–525 (2014).
4. Clarke, T. M. et al. Charge carrier mobility, bimolecular recombination and trapping in polycarbazole copolymer: fullerene (PCDTBT: PCBM) bulk heterojunction solar cells. *Org. Electron.* **13**, 2639–2646 (2012).
5. Nicolai, H. et al. Unification of trap-limited electron transport in semiconducting polymers. *Nat. Mater.* **11**, 882–887 (2012).
6. Armin, A. et al. Simultaneous enhancement of charge generation quantum yield and carrier transport in organic solar cells. *J. Mater. Chem. C* **3**, 10799–10812 (2015).
7. Wetzelaer, G.-J. A. et al. Asymmetric electron and hole transport in a high-mobility n-type conjugated polymer. *Phys. Rev. B* **86**, 165203 (2012).
8. Chua, L.-L. et al. General observation of n-type field-effect behaviour in organic semiconductors. *Nature* **434**, 194–199 (2005).
9. Meijer, E. et al. Solution-processed ambipolar organic field-effect transistors and inverters. *Nat. Mater.* **2**, 678–682 (2003).
10. Armin, A., Jansen-van Vuuren, R. D., Kopidakis, N., Burn, P. L. & Meredith, P. Narrowband light detection via internal quantum efficiency manipulation of organic photodiodes. *Nat. Commun.* **6**, 6343 (2015).
11. Lin, Q., Armin, A., Burn, P. L. & Meredith, P. Filterless narrowband visible photodetectors. *Nat. Photon.* **9**, 687–694 (2015).
12. Tuladhar, S. M. et al. Ambipolar charge transport in films of methanofullerene and poly (phenylenevinylene)/methanofullerene blends. *Adv. Funct. Materi.* **15**, 1171–1182 (2005).
13. Armin, A. et al. Balanced carrier mobilities: not a necessary condition for high-efficiency thin organic solar cells as determined by MIS-CELIV. *Adv. Energy Mater.* **4**, 1300954 (2014).
14. Mozer, A. J. et al. Time-dependent mobility and recombination of the photoinduced charge carriers in conjugated polymer/fullerene bulk heterojunction solar cells. *Phys. Rev. B* **72**, 035217 (2005).
15. Pacios, R., Nelson, J., Bradley, D. D. & Brabec, C. J. Composition dependence of electron and hole transport in polyfluorene:[6, 6]-phenyl C61-butyric acid methyl ester blend films. *Appl. Phys. Lett.* **83**, 4764–4766 (2003).
16. Anthopoulos, T. D. et al. Solution processible organic transistors and circuits based on a C 70 methanofullerene. *J. Appl. Phys.* **98**, 054503–054506 (2005).
17. Irfan, I., Turinske, A. J., Bao, Z. & Gao, Y. Work function recovery of air exposed molybdenum oxide thin films. *Appl. Phys. Lett.* **101**, 093305 (2012).
18. Lin, H. et al. MoO_x as an Efficient and Stable Back Contact Buffer for Thin Film CdTe Solar Cells. *MRS Online Proceedings Library Archive*, 1447 (2012).
19. Armin, A. et al. Spectral dependence of the internal quantum efficiency of organic solar cells: effect of charge generation pathways. *J. Am. Chem. Soc.* **136**, 11465–11472 (2014).
20. Shrotriya, V., Li, G., Yao, Y., Chu, C.-W. & Yang, Y. Transition metal oxides as the buffer layer for polymer photovoltaic cells. *Appl. Phys. Lett.* **88**, 073508 (2006).
21. Armin, A. et al. Electro-optics of conventional and inverted thick junction organic solar cells. *ACS Photonics* **2**, 1745–1754 (2015).
22. Armin, A. et al. Efficient, large area, and thick junction polymer solar cells with balanced mobilities and low defect densities. *Adv. Energy Mater.* **5**, 1401221 (2015).
23. Kaake, L. G., Sun, Y., Bazan, G. C. & Heeger, A. J. Fullerene concentration dependent bimolecular recombination in organic photovoltaic films. *Appl. Phys. Lett.* **102**, 133302 (2013).
24. Burke, T. M. & McGehee, M. D. How high local charge carrier mobility and an energy cascade in a three-phase bulk heterojunction enable >90% Quantum Efficiency. *Adv. Mater.* **26**, 1923–1928 (2014).
25. Bartelt, J. A. et al. The importance of fullerene percolation in the mixed regions of polymer–fullerene bulk heterojunction solar cells. *Adv. Energy Mater.* **3**, 364–374 (2013).
26. Cornil, J., Brédas, J. L., Zaumseil, J. & Sirringhaus, H. Ambipolar transport in organic conjugated materials. *Adv. Mater.* **19**, 1791–1799 (2007).
27. Bässler, H. Charge transport in disordered organic photoconductors a Monte Carlo simulation study. *Phys. Status Solidi (B)* **175**, 15–56 (1993).
28. Parris, P., Kenkre, V. & Dunlap, D. Nature of charge carriers in disordered molecular solids: Are polarons compatible with observations? *Phys. Rev. Lett.* **87**, 126601 (2001).
29. Armin, A., Velusamy, M., Burn, P. L., Meredith, P. & Pivrikas, A. Injected charge extraction by linearly increasing voltage for bimolecular recombination studies in organic solar cells. *Appl. Phys. Lett.* **101**, 083306 (2012).